Fusion Engineering and Design 89 (2014) 2499–2503

Contents lists available at ScienceDirect

Fusion Engineering and Design

journal homepage: www.elsevier.com/locate/fusengdes

Benchmarking of CAD-based SuperMC with ITER benchmark model

Jing Song[a,b], Guangyao Sun[a,b], Zhenping Chen[a,b], Huaqing Zheng[b], Liqin Hu[a,b,*]

[a] University of Science and Technology of China, Hefei, Anhui 230027, China
[b] Institute of Nuclear Energy Safety Technology, Chinese Academy of Sciences, Hefei, Anhui 230031, China

ARTICLE INFO

Article history:
Received 2 March 2014
Received in revised form 28 April 2014
Accepted 12 May 2014
Available online 14 July 2014

Keywords:
ITER
Monte Carlo
CAD
SuperMC
MCNP

ABSTRACT

Neutronics design and analysis of fusion reactors is significantly complex mainly on geometry and physical process of neutron. The great challenges brought by advanced nuclear energy system promote the development of Super Monte Carlo Calculation Program for Nuclear and Radiation Process (SuperMC). The ITER benchmark model, a verification model created by ITER International Organization, was used for benchmarking the latest SuperMC which can perform CAD-based neutron and photon transport calculation. The calculation results of SuperMC for the first wall, divertor cassettes, inboard toroidal field coils and equatorial port were compared with the results of MCNP and the results were coincident. The intelligence and advantage of SuperMC on automatic conversion from complicated CAD model to full format calculation model, complex source construction and geometry description method was demonstrated. The correctness of neutron and photon transport in energy range corresponding to fusion reactors was also demonstrated.

1. Introduction

Compared to ordinary nuclear energy system, neutronics design and analysis of fusion reactors is significantly complex mainly due to the complicated and large scale geometry for modeling, as well as strong anisotropy, large energy range and complex energy spectrum structure of neutrons in fusion reactors. Monte Carlo (MC) methods have obvious advantages to deal with such heterogeneous and complex system. Besides neutronics of fusion reactors, the development of advanced nuclear energy system brings great challenges to current simulation methods and tools of nuclear energy system on neutronics, fluids and heat transfer, materials, fuels, etc. and also computer technology such as geometrical modeling, data visualization and high-performance computing [1–7]. Mainly for accommodating to the demand of advanced nuclear energy system, Super Monte Carlo Calculation Program for Nuclear and Radiation Process (SuperMC) is under development by the FDS Team in China.

It has been recognized that automated translation or direct geometry utilization of CAD model is efficient to alleviate difficulties in the tedious, labor-intensive and error-prone process of describing complicated MC geometries and enhance the capability of dealing with complicated geometry structure [8], especially for fusion reactors. Based on the previous research experience of the FDS Team [9–16] on CAD model conversion, SuperMC 2.1, the latest version, has been developed. It can perform neutron and photon transport calculation based on hybrid MC-deterministic method and ordinary reactor design parameters calculation. The bi-directional automatic conversion between general CAD models and calculation models can be performed. Results and process of simulation can be visualized with dynamical 3D dataset and geometry model [17]. Self-developed continuous-energy cross section data library HENDL [18,19] is available to support the simulation.

ITER benchmark model, created by ITER International Organization, was used for testing and comparison of CAD/Monte Carlo codes developed by different institutes and universities [8]. In order to verify and demonstrate SuperMC's capability of dealing with complex fusion reactor, especially for the intelligence and advantage on complicated geometry processing and correctness of neutron and photon transport simulation in energy range corresponding to fusion reactors, the ITER benchmark model was used for testing SuperMC after series of previous benchmarking [20]. The results of SuperMC were compared with MCNP, whereas the results of MCNP [21] using MCAM [9–16] for converting input model have been compared with the results of other institutions [8,10].

In Section 2, the method of geometry processing and transport simulation of neutron and photon in SuperMC2.1 was introduced. The ITER benchmark model, modeling method and comparison of

* Corresponding author at: University of Science and Technology of China, Hefei, Anhui 230027, China.
E-mail address: liqin.hu@fds.org.cn (L. Hu).

http://dx.doi.org/10.1016/j.fusengdes.2014.05.003
0920-3796/

SuperMC2.1 with MCNP was introduced in Sections 3 and 4. Then calculation results were presented and compared in Section 5.

2. Method of geometry processing and transport simulation of neutron and photon

CAD models represented by Boundary Representation (BREP) [22] can be automatically converted to MC calculation geometry models which are presented hierarchically by primitive solids based on Constructive Solid Geometry (CSG) method. Such approach can significantly reduce the manpower and enhance reliability for constructing the calculation geometry. Hierarchy information of geometry including repeated structure is assigned to support geometry processes during particles transport. Users can fix possible existing errors, create 3D geometry models and interactively and graphically edit physical attributes of materials, sources and tallies. During this conversion, CAD solids are firstly decomposed into convex solids and then presented by intersections of the surfaces wrapping the convex solids. Then each surface is presented by primitive solid which would at last hierarchically present the whole solid. To simplify the geometries, the primitive solids are confined to the minimum size and similar primitive solids are concluded into one. Inversely, inversion from calculation model to CAD model for visualization to locate the defects and errors and further update will accelerate the redesign process. It works by sequentially parsing the calculation model, constructing CSG tree, making primitive solids and building the real solids from the bottom to the top of the CSG tree.

Hierarchical tree structure used for supporting geometry navigation during particles transport process is adopted to describe geometry containing materials. The main geometry classes in SuperMC2.1 are: entity, volume, component and lattice. Volumes are geometry domains defined by Boolean operation of general entities (primitive bodies and auxiliary surfaces). The layout of components consisted of multiple volumes assigned with different materials can be further specified hierarchically respect to other components according to the loading pattern. Through this hierarchical definition, the repeated structure geometry can be easily specified by component and lattice. Additionally, a cuboid must be defined as a world volume and the root node of the geometry hierarchy to completely contain all components. Thus it is not needed to define all spatial area such as cavity in some codes using different geometry representation method to avoid particles loss due to the precision of computers. Advanced geometry navigation acceleration methods oriented from computer graphics, such as automatic neighbor search method, oriented bounding box method and 3D space partition method are designed to enhance the efficiency of geometry processing.

For neutron, inelastic scattering, elastic scattering and absorption reaction process from 10^{-11} MeV to 150 MeV are considered. Thermal scattering effect is treated with free-gas approximation model wherein the velocities of the target nuclei obey Maxwellian distribution and separate $S(\alpha, \beta)$ scattering law data which is thermal scattering data of molecules or crystalline materials. Also, Doppler Broadening Rejection Correction (DBRC) method is adopted to treat the scattering of neutron in epithermal energy range. Removal neutrons are considered and separately sampled. Self-shielding effect in the unresolved resonance energy range which has obvious effect on results correctness for problems with an appreciable flux spectrum in unresolved resonance energy range is accurately treated using probability tables. For photons, the code accounts for Compton scattering, coherent scattering, possibility of fluorescent emission after photoelectric absorption, absorption in electron–positron pair production and photonuclear reaction from 1 KeV to 100 GeV.

3. The ITER benchmark model

ITER benchmark model [8] was created by ITER International Organization with CATIA V5 which has been chosen as the CAD system for ITER design, saved into STEP format and used for testing and comparison of CAD/Monte Carlo codes developed by various institutes and universities. This CAD model includes blanket, divertor, vacuum vessel, cryostat, bioshield, central solenoid coils, TF coils, PF coils, lower, upper and equatorial ports, i.e. all the important parts and components of the ITER device are involved as well as various complicated curved surfaces which can fully test the capacity of the neutronics codes. The model is a 40° sector in toroidal direction of the full ITER machine from the central solenoid to the outer magnet coils, 1560 cm in radial direction and 1581 cm in poloidal direction.

Besides the geometric model, the materials, the source distribution and the tallies are also specified in related documents. The plasma chamber is given as CAD model which is also 40° toroidal sector, 1168 cm length and 770.8 cm height. The plasma source is located in a structured cylindrical grid with probability distribution between R–Z grid cells and uniformly distributed in each grid cells within the 40° of the problem bounds.

4. Modeling method and comparison of SuperMC2.1 with MCNP

Four categories of results should be calculated and compared: the neutron wall loading (NWL) on the first wall, the neutron flux and nuclear heating in divertor cassettes, the nuclear heating in the inboard toroidal field (TF) coils and the flux in the equatorial ports. Calculation results of SuperMC2.1 and MCNP were compared using the same fusion nuclear data library FENDL 2.1 [23]. ENDF/B-VI [24] was used as alternatives for missing isotope Ba 138. 40° toroidal segment of the full ITER model with reflected boundary surfaces was used for benchmarking.

Original geometry files released by ITER including 14 subsystems of ITER device and plasma source part are all in STEP format. For MCNP calculation, STEP format CAD models were automatically converted to input file of MCNP with MCAM which is also developed by the FDS Team. Some reasonable and necessary modifications of CAD models had been performed in previous verification work of MCAM with ITER benchmark model [10]. In this verification, the material properties were assigned graphically to group geometries according to the material definition file given by ITER International Organization. The plasma source was described in FORTRAN subroutine source code files of MCNP. An international calculation results comparison had been carried out between different codes and the analysis results showed good agreement [8]. The same modification methods of geometry during the conversion of CAD models were adopted in the benchmarking of SuperMC. Geometry, materials properties, source distribution and tally settings were modeled completely in graphic user interface for benchmarking SuperMC, as shown in Fig. 1.

In testing with ITER benchmark model, the major differences between SuperMC 2.1 and MCNP are following: (1) Generally, SuperMC 2.1 directly starts from importing CAD models and converts geometry internally for further particles transport calculation while MCNP calculation starts from the ASCII text input file. The physical properties including materials, sources and tallies can be assigned and converted in SuperMC. In the benchmarking process, the input file of MCNP was automatically converted from the same CAD models with MCAM. (2) Complex spatial distribution of sources such as plasma source in ITER benchmark model can be converted from CAD model and probability distribution can be assigned in visualized and interactive manner. Then the source configuration can be converted internally for further transport calculation in

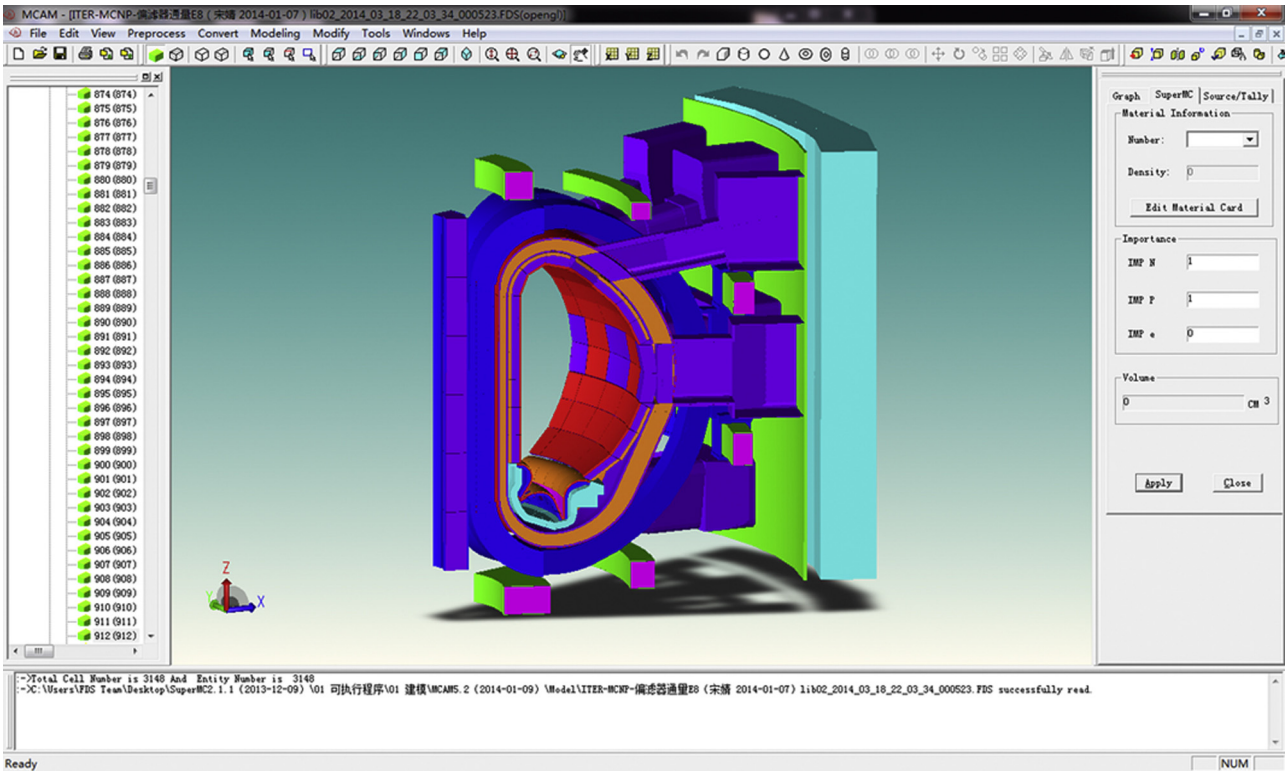

Fig. 1. ITER benchmark model in SuperMC.

SuperMC 2.1. However, source subroutine is necessary for problems of complex source distribution and should be compiled with other source codes in MCNP. (3) SuperMC 2.1 adopts hierarchical solid geometry description method assisted with surface description method while MCNP mainly adopts surface description method. It is an advantage of SuperMC that there is no need to describe or convert cavity cells so that particles loss due to the precision of computers is avoided.

5. Calculation results

5.1. Neutron wall loading on the first wall

Since the neutron wall loading is energy current density of uncollided and scattered neutrons on the first wall, this case serves to compare the correctness and ability to model the plasma source and the first wall geometry. The plasma-facing surface of the ITER benchmark model was divided into 18 modules and numbered in the poloidal direction, starting on the lower inboard side, moving up the inboard side and finishing at the bottom of the outboard side. Then each module was divided into 4 pieces. The calculation results of SuperMC2.1 and MCNP on 72 distinct surfaces were listed by module number in Fig. 2. The average deviation of NWL between SuperMC and MCNP was 0.00071% (from 0% to 0.00268%) and the average standard error for all segments was 0.0016 (from 0.0012 to 0.0022).

5.2. Neutron flux and nuclear heating in divertor cassettes

Neutron flux and nuclear heating in the structural elements of the divertor cassette were calculated to test the capability to model complex geometry and neutron responses in those objects. As in Fig. 3, outer vertical W, outer vertical CFC, inner vertical CFC, inner vertical W and cassette body of the divertor cassettes are marked as Group 1-Group 5. Each group is divided into 7 segments numbered 1–7. The neutron flux was calculated for four energy groups ($E < 1$ eV, 1 eV–0.1 MeV, 0.1–1 MeV, 1–20 MeV) and the total ($E < 20$ MeV). The nuclear heating in the structural elements of the cassette was calculated. The calculation results of total neutron flux and total nuclear heating of neutron and photon were shown in Figs. 4 and 5 separately. The average deviation of total neutron flux value between SuperMC and MCNP was 0.00218% (from 0% to 0.00983%) and the average standard error for all segments was 0.0025 (from 0.0014 to 0.0049). The average deviation of nuclear heating value was 0.00303% (from 0% to 0.01037%) and the average standard error was 0.0058 (from 0.0030 to 0.0118). It is clear from the calculation results that neutron flux in inner vertical W of the divertor cassette which faces to the plasma directly and is nearest from the plasma is higher than other parts.

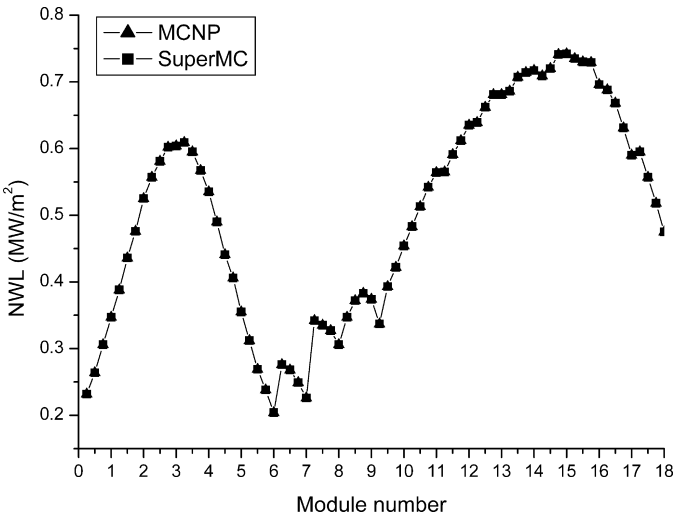

Fig. 2. Neutron wall loading for ITER benchmark model.

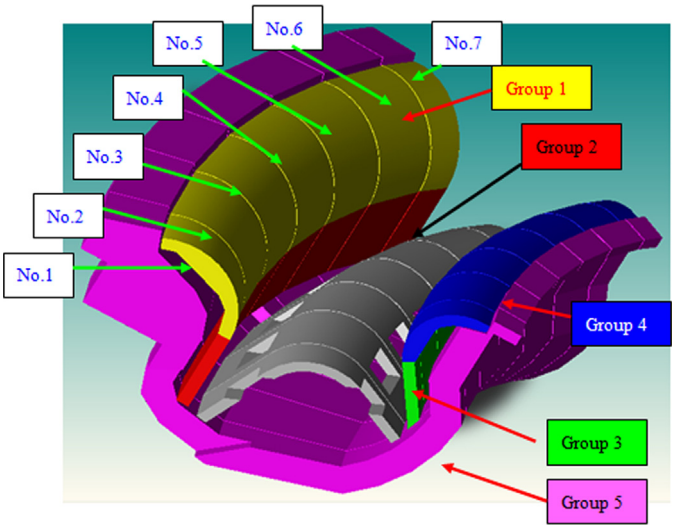

Fig. 3. Divertor cassettes model.

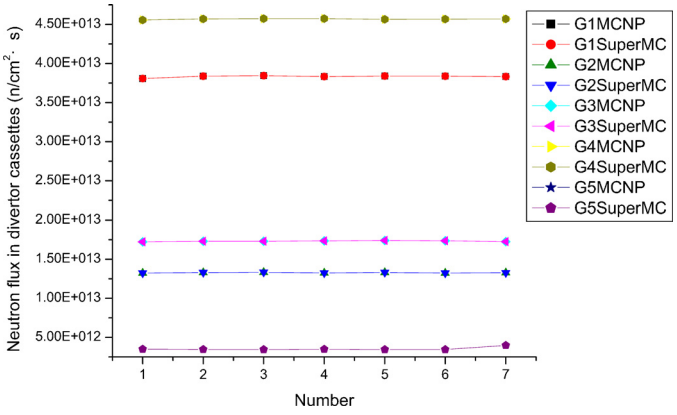

Fig. 4. Neutron flux in divertor cassettes.

5.3. Nuclear heating in the inboard TF coils

A majority of neutrons and the photons are shielded by blankets and vacuum vessel before they reach the inboard toroidal field coils. The total amount of nuclear heating in these magnet coils is one of the engineering limits of the ITER design. The axial profile of the neutron, photon and total nuclear heating in the 10 uniformly cut legs of inboard toroidal field coils were specified to test the

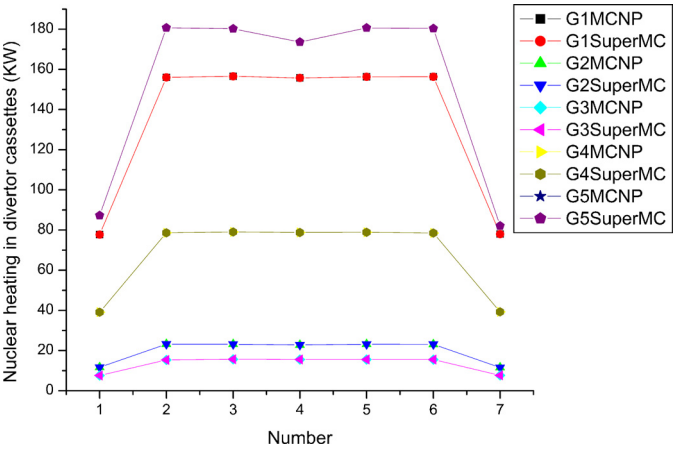

Fig. 5. Nuclear heating in divertor cassettes.

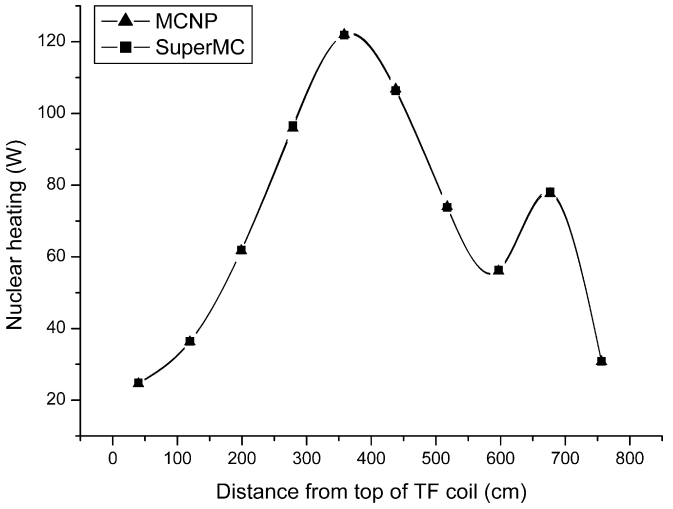

Fig. 6. Axial profile of the total nuclear heating in inboard toroidal field coils.

calculation ability on the capability of the thick shielding. The total nuclear heating of the 10 segments was calculated and compared as in Fig. 6. The vertical axial standard for segments sequence from bottom to top. The average deviation of nuclear heating value between SuperMC and MCNP was 0.47198% (from 0.13050% to 0.83210%) and the average standard error for all segments was 0.0757 (from 0.0539 to 0.1132). The total nuclear heating was 685.78 W.

5.4. Flux in the equatorial ports

The fluxes in the void space behind the equatorial port plugs and shield involve multiple scattering events and deep penetration. The tally zones in equatorial port were shown in Fig. 7. Neutron flux in four energy groups (<1 eV, 1 eV–0.1 MeV, 0.1–1 MeV, 1–20 MeV) and total (<20 MeV) neutron flux were calculated for radial segments (5 cm interval) of the dummy port plug and the shield plug, averaged over the poloidal height and the toroidal width. 7 by 3 small tally spheres have been placed in equatorial ports as for calculating the neutron and photon fluxes to test the ability to simulate the effect of streaming along gaps in the geometry. The neutron flux in 10 by 3 segments of shield plug located at left, middle and

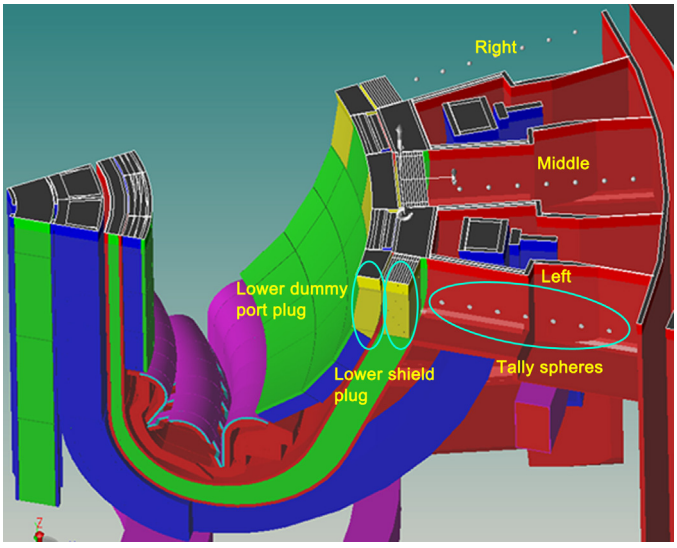

Fig. 7. Tally zones in the equatorial ports.

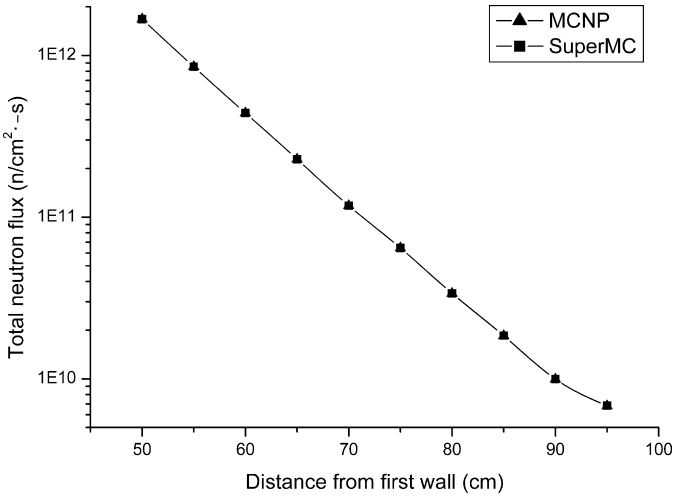

Fig. 8. Neutron flux in the equatorial ports.

right position were calculated and compared. The average deviation between SuperMC and MCNP for all segments was 0.07422% (from 0% to 0.74243%) and the average standard error was 0.0301 (from 0.0040 to 0.0800). The results at the middle position were shown in Fig. 8.

6. Conclusion and prospect

The benchmarking with complex ITER benchmark model demonstrated SuperMC2.1's intelligence and advantage on automatic conversion from complicated CAD model to full format calculation model, complex source construction, geometry description method. The four categories of calculation results of SuperMC were consistent with the results of MCNP within the statistical uncertainty inherent in the MC method. The correctness of neutron and photon transport in energy range corresponding to fusion reactor in SuperMC was successfully demonstrated. In the future, besides ITER benchmark model, the latest ITER model for neutronics design and analysis will be used for benchmarking of SuperMC with the development of more efficient variance reduction techniques for shielding problem of fusion reactors.

Acknowledgements

This work was supported by the Strategic Priority Research Program of Chinese Academy of Sciences (No. XDA03040000), the National Natural Science Foundation of China (No. 91026004).

References

[1] P. Finck, D. Keyes, R. Stevens, Workshop on Simulation and Modeling for Advanced Nuclear Energy Systems, Washington, DC, 2006.
[2] G. Palmiotti, J. Cahalan, P. Pfeiffer, T. Sofu, T. Taiwo, T. Wei, et al., Requirements for Advanced Simulation of Nuclear Reactor and Chemical Separations Plants, Argonne National Laboratory, ANL-AFCI-168, 2005.
[3] W.R. Martin, Challenges and prospects for whole-core Monte Carlo analysis, Nucl. Eng. Technol. 44 (2) (2012) 151–160.
[4] N.Z. Cho, J. Chang, Some outstanding problems in neutron transport computation, Nucl. Eng. Technol. 41 (4) (2009) 381–390.
[5] K. Smith, B. Forget, Challenges in the development of high-fidelity LWR core neutronics tools, in: M&C 2013, Sun Valley, Idaho, 2013.
[6] P.J. Turinsky, Advances in multi-physics and high performance computing in support of nuclear reactor power systems modeling and simulation, Nucl. Eng. Technol. 44 (2) (2012) 103–112.
[7] F.B. Brown, Recent advances and future prospects for Monte Carlo, Prog. Nucl. Sci. Technol. 2 (2011) 1–4.
[8] P.P.H. Wilson, R. Feder, U. Fischer, M. Loughlin, L. Petrizzi, Y. Wu, et al., State-of-the-art 3-D radiation transport methods for fusion energy systems, Fusion Eng. Des. 83 (2008) 824–833.
[9] Y. Wu, FDS Team, CAD-based interface programs for fusion neutron transport simulation, Fusion Eng. Des. 84 (2009) 1987–1992.
[10] Y. Li, L. Lu, A. Ding, H. Hu, Q. Zeng, S. Zheng, et al., Benchmarking of MCAM 4.0 with ITER 3D model, Fusion Eng. Des. 82 (15) (2007) 2861–2866.
[11] Q. Zeng, L. Lu, A. Ding, Y. Li, H. Hu, S. Zheng, et al., Update of ITER 3D basic neutronics model with MCAM, Fusion Eng. Des. 81 (23/24) (2006) 2773–2778.
[12] H. Hu, Y. Wu, M. Chen, Q. Zeng, A. Ding, S. Zheng, et al., Benchmarking of SNAM with the ITER 3D model, Fusion Eng. Des. 82 (15–24) (2007) 2867–2871.
[13] P.C. Long, J. Zou, S.Q. Huang, Y.F. Qiu, Development and application of SN auto-modeling tool SNAM 2.1, Fusion Eng. Des. 85 (7–9) (2010) 1113–1116.
[14] G.Z. Wang, J. Xiong, P.C. Long, D.X. Wang, K. Zhao, Q. Zeng, et al., Progress and applications of MCAM: Monte Carlo automatic modeling program for particle transport simulation, Prog. Nucl. Sci. Technol. 2 (2011) 821–825.
[15] Y. Wu, Y. Li, L. Lu, A.P. Ding, H.M. Hu, Q. Zeng, et al., Research and development of the automatic modeling system for Monte Carlo particle transport simulation, Chin. J. Nucl. Sci. Eng. 26 (1) (2006) 20–27.
[16] Y. Wu, X.G. Xu, The need for further development of CAD/MCNP interface codes, Trans. Am. Nucl. Soc. 96 (2007) 392–394.
[17] Y.T. Luo, P.C. Long, G.Y. Wu, Q. Zeng, L.Q. Hu, J. Zou, et al., SVIP-N 1.0: an integrated visualization platform for neutronics analysis, Fusion Eng. Des. 85 (7–9) (2010) 1527–1530.
[18] J. Zou, Z.Z. He, Q. Zeng, Y.F. Qiu, M.H. Wang, Development and testing of multi group library with correction of self-shielding effects in fusion–fission hybrid reactor, Fusion Eng. Des. 85 (7–9) (2010) 1587–1590.
[19] D.Z. Xu, Z.Z. He, J. Zou, Q. Zeng, Production and testing of HENDL-2.1/CG coarse-group cross-section library based on ENDF/B-VII.0, Fusion Eng. Des. 85 (10–12) (2010) 2105–2110.
[20] G.Y. Sun, J. Song, H.Q. Zheng, Benchmark of neutron transport simulation capability of Super Monte Carlo Calculation Program SuperMC 2.0, Atom. Eng. Sci. Technol. 47 (2013) 520–525 (in Chinese).
[21] [5X-]Monte Carlo Team, MCNP – A General Monte Carlo N-Particle Transport Code, Version 5 – vol. I: Overview and Theory, LA-UR-03-1987, 2005.
[22] A.A.G. Requicha, Representations for rigid solids: theory methods and systems, ACM Comput. Surv. 12 (4) (1980) 437–464.
[23] The IAEA Nuclear Data Section, FENDL-2.1 Fusion Evaluated Nuclear Data Library, INDC (NDS)-467, Vienna, Austria, 2004, December.
[24] J.S. Hendricks, S.C. Frankle, J.D. Court, ENDF/B-VI data for MCNP, and Errata, Los Alamos National Laboratory Report LA-12891, 1994.